Sub-picosecond electron and phonon dynamics in nickel

2005 J. Phys.: Condens. Matter 17 6823

(http://iopscience.iop.org/0953-8984/17/43/004)

INSTITUTE OF PHYSICS PUBLISHING JOURNAL OF PHYSICS: CONDENSED MATTER

J. Phys.: Condens. Matter **17** (2005) 6823–6834 doi:10.1088/0953-8984/17/43/004

Sub-picosecond electron and phonon dynamics in nickel

M van Kampen[1,2,4], J T Kohlhepp[1], W J M de Jonge[1], B Koopmans[1] and R Coehoorn[3]

[1] Department of Applied Physics, Center for NanoMaterials and COBRA Research Institute, Eindhoven University of Technology, PO Box 513, 5600 MB Eindhoven, The Netherlands
[2] IMEC, Kapeldreef 75, 3001 Heverlee, Belgium
[3] Philips Research Laboratories, Professor Holstlaan 4, NL-5656 AA, Eindhoven, The Netherlands

E-mail: vkampen@imec.be

Received 8 June 2005, in final form 30 August 2005
Published 14 October 2005
Online at stacks.iop.org/JPhysCM/17/6823

Abstract

Electron thermalization and electron–phonon relaxation in metals can be studied by measuring the transient change in sample reflectivity after excitation with a femtosecond laser pulse. This paper describes experiments on ferromagnetic nickel thin films, in particular addressing the analysis of the reflectivity data and its dependence on temperature. Specifically engineered samples of optically thin films on a thermally insulating barrier layer are used to minimize heat diffusion and hot-electron transport out of the volume under consideration. It is found that lattice expansion and strain wave phenomena significantly contribute to the transient reflectivity, and therefore have to be accounted for when determining the electron–phonon relaxation time. The measurements reveal an electron thermalization time of 80 fs, and an electron–phonon energy relaxation time of 0.3–0.4 ps.

After laser heating of a metallic system, electron–electron (e–e) and electron–phonon (e–p) interactions give rise to an ultrafast reestablishment of an equilibrium situation, typically within only a few picoseconds. This ultrafast electron dynamics is well studied in noble metals as gold and silver, both theoretically as well as experimentally [1–4]. These sp-like materials serve as a model system, and are well described by the Fermi liquid theory. In contrast, much less is known about the electron dynamics in (ferromagnetic) transition metals. Ni is a typical ferromagnetic 3d transition metal, with strongly peaked d-bands close to the Fermi level. A detailed study of the ultrafast carrier dynamics in the 3d elementary metals—in particular the comparison with noble metals—is considered a very relevant issue serving our fundamental understanding of the dynamics in metallic systems in general. An equally

[4] Author to whom any correspondence should be addressed.

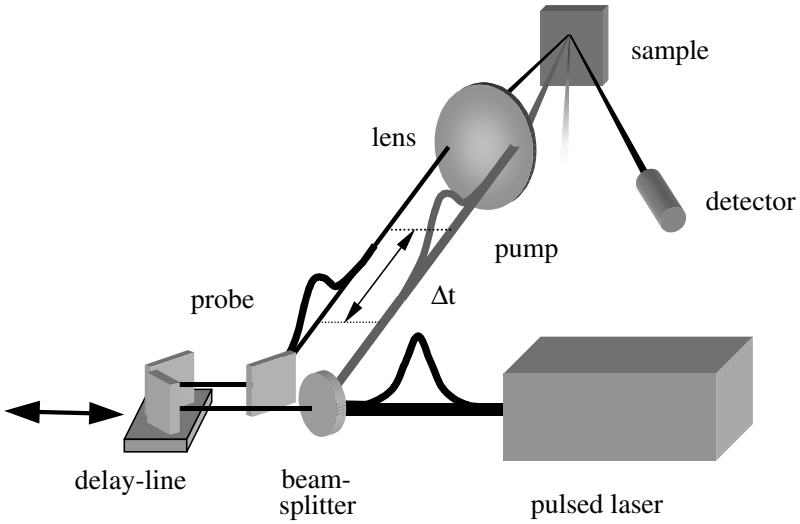

Figure 1. Schematic pump–probe setup. The time-delay between pump- and probe-pulse is controlled by varying the optical path with a delay line. The intensity of the reflected probe is related to the electron distribution.

important motivation is provided, however, by its relevance for the interpretation of the sub-picosecond magnetization dynamics that has recently been explored [5] and has become one of the most intriguing research issues in magnetism today [5–8]

In all-optical pump–probe experiments studying the electron dynamics, the transient change in electron occupation as induced by an intense pump pulse (typically shorter than 100 fs) is probed by measuring the intensity after reflection of the sample of a second (probe) laser pulse that follows the pump at a variable delay Δt, as illustrated in figure 1. Studies of the magnetization dynamics, using similar, magneto-optic pump–probe techniques, have revealed that the magneto-optical contrast of ferromagnetic metals such as nickel and cobalt is (partially) quenched within hundreds of femtoseconds after sudden laser heating. Although care has to be taken in properly interpreting these data, in particularly being aware of the role of spin-selective state-filling effects [7, 9], it has been demonstrated unambiguously that a genuine loss in magnetic order occurs at a surprisingly small timescale of at most a few hundred femtoseconds. Little is known so far about the microscopic mechanism underlying the ultrafast demagnetization. Obviously, measuring and understanding the e–e and e–p interactions triggered by the laser heating will be one of the prerequisites for a further development of our insight in the magnetic processes.

During the past years, several reports have addressed the e–e and e–p dynamics in ferromagnetic 3d metals. Although all studies agree on a fast energy equilibration of the electron and phonon system in the (sub)ps range, a surprisingly large scattering of values for seemingly analogous structures can be witnessed. Taking nickel as an exemplary case, values reported for the e–p relaxation time range from ∼0.5 to 1.5 ps. Obviously, the field of carrier and spin dynamics will profit considerably from formulating a more coherent view.

In this paper we report on pump–probe investigations on specifically engineered nickel thin-film systems. By considering films thinner than the optical penetration depth (∼15 nm), grown on a thermally insulating 'barrier', a more direct view on the dynamics is achieved [10]. In particular, the insulating layer blocks hot-electron transport and significantly reduces thermal diffusion out of the heated film on a picosecond timescale. Moreover, a careful analysis of the

data, including an analysis of shock wave phenomena, is considered to provide a major step towards an unambiguous understanding.

This paper is organized as follows. In section 1 we review the basic theory of e–e and e–p interactions. The experimental approach and preparation of samples is presented in section 2. Experimental results for various nickel structures are presented in section 3. A detailed comparison with other work is discussed in section 4.

1. Theory

Upon absorption of a short laser pulse electrons are excited from the occupied states below the Fermi level to the empty states above. The optical excitation creates a non-equilibrium distribution of highly energetic electrons, with energies ranging up to the photon energy ($\hbar\nu \approx 1.6$ eV in our experiments) above the Fermi level. The lattice, on the other hand, is initially undisturbed. In the subsequent relaxation processes the energetic electrons thermalize to a Fermi–Dirac distribution by e–e scattering and the lattice is heated by e–p scattering.

1.1. Electron–electron scattering

Considering only e–e scattering, the lifetime of a single, highly excited electron in a free-electron metal is given by [1]

$$\tau_{ee}(E) = \frac{1}{K_{ee}(E - E_F)^2}, \tag{1}$$

with $1/K_{ee} \approx 35$ fs eV^2 for Ag [3, 11] and $\approx$3 fs eV^2 for Ni [3, 16]. Equation (1) is only a rough approximation for Ni. In Ni the d-bands intersect with the Fermi level, causing deviations of the measured lifetimes from the free-electron behaviour [3]. In particular, the lifetime of electrons close to E_F is strongly reduced compared to equation (1). The d-bands provide extra phase-space for scattering, causing up to a ten-fold reduction in scattering times compared to Ag.

After optical excitation, the combined effect of many e–e scattering events leads to the thermalization of the electron gas. The thermalization time t_{th} depends on the e–e scattering constant K_{ee} and the electron temperature T_e. Different analytical approximations [1, 12, 16] for the thermalization process lead to an expression of the form

$$t_{th} = \frac{A}{K_{ee}T_e^2} \tag{2}$$

with, for Ni, $A = 6.7 \times 10^{-7}$ [1], 1.9×10^{-7} [12] and 2.2×10^{-7} K^2 eV^{-2} [16]. Taking $A = 2 \times 10^{-7}$ K^2 eV^{-2}, $1/K_{ee} = 3$ fs eV^2 and $T_e = 400$ K, a thermalization time of $\sim$300 fs is found for Ni. As was pointed out above, the lifetime of low-energy electrons in Ni is shorter than that given by (1). The actual electron thermalization in Ni is therefore expected to proceed faster.

1.2. Electron–phonon scattering

The lifetime of highly excited electrons is dominated by e–e scattering. However, when their energy gets closer to E_F, τ_{ee} becomes much longer and e–p scattering processes start to dominate. Collisions between electrons and phonons transfer energy between the electron and lattice system, equilibrating the temperature of both systems.

When both the electron system and the phonon system are in internal thermal equilibrium, the energy transfer between the two systems is approximately linear in their temperature difference $T_e - T_l$ [12, 16]. In the two-temperature model (2TM) [1] this relation is used

to model the dynamics by two coupled differential equations, describing respectively the time-evolution of the electron temperature and the phonon temperature. Assuming that the heat capacity of both the electron (c_e) and phonon (c_l) systems is sufficiently temperature independent, $T_e(t)$ and $T_l(t)$ will show an exponential time dependence and approach a common value for $t \to \infty$.

In actual pump–probe experiments the interpretation is more complex, since the electron system is initially not in internal thermal equilibrium. One solution is to consider only the regime where the electron system is thermalized, i.e. ignore the first few hundreds of femtoseconds after excitation. Alternatively, the electron temperature transient can be described by the empirical relation [2, 14]

$$\Delta T_e(\Delta t) = \Delta T_1 \left[1 - \exp(-\Delta t/\tau_{th})\right] \exp(-\Delta t/\tau_E) + \Delta T_2 \left[1 - \exp(-\Delta t/\tau_E)\right], \quad (3)$$

with τ_{th} the (characteristic) thermalization time, ΔT_2 the rise of the electron (and lattice) temperature after e–p relaxation and ΔT_1 the rise of the electron temperature in the absence of e–p relaxation. Note that the definition of an 'electron temperature' when the system is not in equilibrium is non-trivial. We adopted the common convention of relating T_e to the slope of the electron distribution at the Fermi level. The e–p relaxation is described by an exponential decay with time constant τ_E (where the subscript E denotes the energy relaxation of the electron gas), a form that can be derived from the 2TM. We verified equation (3) by comparison with the numerical solution of the Boltzmann equations that describe the time evolution of an electron distribution coupled to a phonon bath [16], an approach that also captures the initial non-equilibrium dynamics. In this paper, equation (3) will be used to determine the electron thermalization time and the e–p relaxation time. To correct for the finite duration of the laser pulses, the transient as given by equation (3) is broadened by convolution with a Gaussian pulse profile.

2. Experimental details

All experiments were performed on Ni thin-film samples. In order to reduce hot (ballistic) electron transport and heat diffusion out of the laser irradiated volume, we mainly focus on samples with a thermally insulating substrate with a relatively high bandgap, e.g. Si/Si_3N_4 (60 nm)/Ni(10 nm)/Cu(3 nm). The Ni layer is chosen optically thin and is therefore uniformly heated, and Si_3N_4 acts as the electrically and thermally insulating layer. The thin Cu capping serves to prevent Ni from oxidizing. In this work an all-metallic wedge-structure is also studied, i.e. Cu(001)/Ni(001)(0–30 nm)/Cu(3 nm).

The electron dynamics is probed by time-resolved reflectometry and ellipsometry. We used a pump–probe configuration, described in detail in [15] and depicted in figure 1, to measure the transient reflective properties of the film. In the pump–probe scheme, the material is first excited by an intense laser 'pump' pulse. A much weaker 'probe' pulse, which follows the pump at a variable time-delay, is used to measure the change in reflectivity.

When measuring the transient reflectivity, the pump beam is modulated with a chopper and the induced intensity changes in the reflected probe are detected using a lock-in scheme. This technique simply yields an intensity change proportional to the change in reflectivity, ΔR. The interpretation of these reflectivity transients is well established for noble metals, showing $\Delta R \propto\sim \Delta T_e$ for photon energies close to the interband transition threshold (ITT), i.e. using a resonant probe, and ΔR proportional to the excess energy in the electron system for photon energies far from the ITT [1] (off-resonance). The analysis in the case of 3d-metals is potentially much more complicated due to the d-bands intersecting with or lying close to the Fermi level. However, since our $\Delta R(t)$ data (discussed in section 3.1) show a delayed

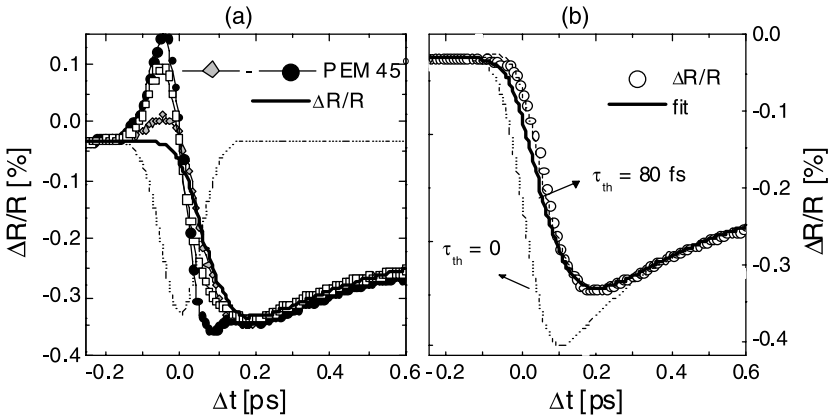

Figure 2. Reflectivity measurements on Si/Si_3N_4 (60 nm)/Ni(10 nm)/Cu(3 nm). (a) Symbols: transients using the PEM technique, showing a change of the coherent effect for different chirp values. Solid line: result using the pump-modulation technique. The dotted line represents the pump–probe cross-correlation. (b) Reflectivity measurement (open circles) and a fit to equation (3) (solid line) excluding the interval $-0.1 < \Delta t < 0.1$ ps. The dotted curve represents equation (3), but with t_{th} put to zero.

response and the temperature rise is limited (∼+200 K), we adapt the usual interpretation of $\Delta R \propto \Delta T_e$ [5, 14].

A complementary view on the transient reflection is provided by an approach that is particularly attractive in cases where a significant amount of pump light is scattered into the detector. By adding a photo-elastic modulator in the probe beam, both pump and probe are modulated. This 'double modulation' allows for a unique separation of the pump-induced changes in the probe reflectivity, and is insensitive to scattered pump light. In [15] this PEM scheme is analysed, showing that it yields an intensity change proportional to a linear combination of changes in r_s and r_p, the reflection coefficients for s and p polarized light.

Since the samples are mounted on a copper holder that is fitted with a resistive heater, temperature-dependent measurements are also possible. Finally, we emphasize that in the analysis of the data, broadening due to the finite length of the laser pulses (85 fs FWHM, $h\nu = 1.6$ eV) has been explicitly taken into account.

3. Results

3.1. Thermalization

Figure 2(a) shows results of transient reflectivity measurements using both techniques (with and without PEM) on a 10 nm Ni film on a Si/Si_3N_4 (60 nm) substrate. In the figure the relative change in reflectivity, $\Delta R/R$, is plotted versus pump–probe delay Δt for the first 0.6 ps. During pump–probe overlap the PEM technique and the direct measurement yield different results. This is related to a coherent process, i.e. a non-linear optical process in which both pump- and probe-photons are involved and that is described by the third-order optical susceptibility. The coherent process is found to affect the polarization of the probe. It is found that the magnitude and shape of the coherent effect depend on the chirp of the laser pulses, an effect that is described in more detail in [16].

After the coherent process the two techniques yield identical results, showing that both methods give the same view on the electron dynamics. In both of the measurements, the

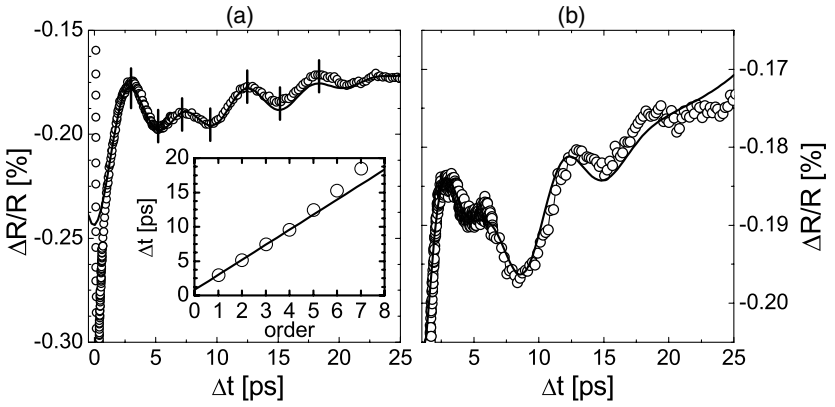

Figure 3. Reflectivity measurements on Si/Si_3N_4 (60 nm)/Ni(10 nm)/Cu(3 nm). (a) Reflectivity transient showing acoustic strain wave effects. The solid line is a fit using two damped sines ($f_1 = 133$ GHz, $f_2 = 194$ GHz) and a linear background. The inset shows the relation between Δt and the extrema indicated by black lines. (b) Transient measured on the same sample, but at a different position. The fit yields $f_1 = 128$ GHz and $f_2 = 192$ GHz.

reflectivity reaches a minimum 190 fs after excitation. The delayed minimum suggests that the method is mainly sensitive to thermalized electrons, i.e. $\Delta R \propto \Delta T_e$. In the case of a high sensitivity to non-thermal electrons, or when measuring the excess energy, an instantaneous response would have been expected.

Combining different reflectivity measurements, the extremum is found at $t_{ex} = 200 \pm 20$ fs, using pulses of 85 fs. This is somewhat faster than other values reported on Ni, e.g. of 260 fs ([5] using 60 fs pulses) and 280 fs ([6] using 150 fs pulses and employing optical second-harmonic generation (SHG) to analyse the dynamics).

Alternatively, we used equation (3), broadened by the pump–probe cross-correlation of 120 fs (FWHM), to describe the reflectivity transients, figure 2(b). The solid line in the figure represents a fit excluding the region showing coherent contributions ($-0.1 < \Delta t < 0.1$ ps). Using a value $\tau_E = 0.32$ ps, which will be discussed in section 3.3, a thermalization time $\tau_{th} = 0.08$ ps is found. The correspondence during pump–probe coincidence is not very good, and the onset of the reflectivity response seems to be shifted to positive delay times. It was carefully checked that $\Delta t = 0$ was correctly determined. Most likely, the coherent contribution is responsible for the observed discrepancy. Fitting with an additional Gaussian contribution with the width of the pump–probe cross-correlation, the dashed curve is found that much better describes the transient data.

3.2. Acoustic strain waves

An important issue after, and even during, e–p relaxation is the effect of the distorted lattice on the reflectivity. Figure 3(a) shows a reflectivity trace for the Si_3N_4/Ni structure up to $\Delta t = 25$ ps. After a rapid e–p relaxation, showing up as a steep drop of $\Delta R/R$ during the first 2 ps, a complex series of oscillations is visible with amplitudes of up to 10% of the initial step around $\Delta t = 0$. It was found that the details of the response depend on the position on the sample, see e.g. figure 3(b), most likely due to inhomogeneities. We stress that the short-term dynamics (<2 ps) was found to be completely homogeneous over the samples.

The wavelike phenomena are related to strain waves in the sample that are caused by the rapid heating. In the Si_3N_4/Ni case, a thin Ni film on top of a transparent layer is uniformly

heated. Si_3N_4 has a lower acoustic impedance than Ni and it can be shown that in this case the surface displacement of the Ni layer is similar to that of a free-standing film. One can thus expect a thickness oscillation with period $2d_{\mathrm{Ni}}/v_{l,\mathrm{Ni}}$, with d_{Ni} the thickness of and $v_{l,\mathrm{Ni}}$ the speed of sound in the Ni layer. The actual sample is capped by an originally 3 nm Cu layer to prevent Ni oxidation. Copper capping will increase the oscillation period, and thus leads to an underestimation of $v_{l,\mathrm{Ni}}$ when using d_{Ni}. The sudden heating of the Ni film will also launch a strain wave in the Si_3N_4. Strain waves in transparent films can be observed in optical experiments since they provide an extra interface for reflection.

In figure 3(a) the extrema of the fast oscillation in $\Delta R/R$ are indicated by vertical lines. The inset shows the position of the extrema versus their order number. The linear slope extracted from the first four points results in $v_l = 4.5$ km s^{-1} ($2d = 20$ nm), close to but somewhat lower than the literature value for the speed of sound in Ni (5 km s^{-1}). Also, the intercept with the y-axis lies at a positive Δt. This is expected since the lattice is heated during e–p relaxation and not directly at $\Delta t = 0$.

The solid lines in figures 3(a) and (b) represent fits assuming a linear background due to diffusive cooling and two damped sines to account for strain wave phenomena. Although this is expected to be a coarse approximation to the lattice dynamics and its effect on the reflectivity, it allows us to determine the main frequency components. The fits show a good correspondence with the observed transients. Moreover, consistently two contributions are found with a ∼5.2 and ∼7.8 ps period, respectively. The 5.2 ps period corresponds to the Ni contribution ($v_l = 3.8$ km s^{-1}), while the slower component is attributed to acoustic strain waves generated in the 60 nm Si_3N_4 layer. This results in a sound velocity of 15 km s^{-1}, in reasonable agreement with the literature value of 11 km s^{-1}.

Altogether, it has to be concluded that lattice effects are of importance in the interpretation of transient reflectivity experiments on Ni thin films. Even when analysing ΔR during the first picoseconds, their contribution cannot be fully neglected. Based on the good correspondence of the two-component fit for $\Delta t > 2$ ps, we believe it a good approximation to extrapolate the fitted curve to the first picoseconds after excitation to make an estimate of the effect of strain waves during e–p relaxation. This procedure will be adopted in the next section.

3.3. *Electron–phonon relaxation*

From the strain wave analysis presented in the previous section, it is clear that the expansion of the lattice also contributes significantly to $\Delta R(\Delta t)$. The lattice expansion is driven by the lattice temperature, which for the uniformly excited film can be approximated by

$$\Delta T_l(t) = \Delta T_\infty \left(1 - \mathrm{e}^{-\frac{t}{\tau_\mathrm{E}}}\right). \tag{4}$$

The expansion of the lattice upon transient heating can in principle be calculated using the equation for thermoelasticity and equation (4). Then, the lattice-induced change in reflectivity should be calculated for the (non-uniform) displacement of the atomic layers.

Here we will employ a more simple model, approximately valid as long as the lattice expansion $\Delta d(t)$ is much smaller than its final equilibrium, $\Delta d(\infty)$. It is assumed that the rate of change of the thickness of the Ni layer is proportional to ΔT_l, i.e. $\mathrm{d}\Delta d(t)/\mathrm{d}t \propto \Delta T_l(t)$, and that the lattice-induced change in reflectivity, ΔR_l, is proportional to Δd. Using equation (4), it then follows that

$$\Delta R_l(t) \propto \Delta d(t) \propto t + \tau_\mathrm{E}\left(\mathrm{e}^{-\frac{t}{\tau_\mathrm{E}}} - 1\right). \tag{5}$$

Note that for $t \gg \tau_\mathrm{E}$, this expression reduces to $\Delta R_l(t) \propto t - \tau_\mathrm{E}$, i.e. a linear expansion delayed by the e–p relaxation.

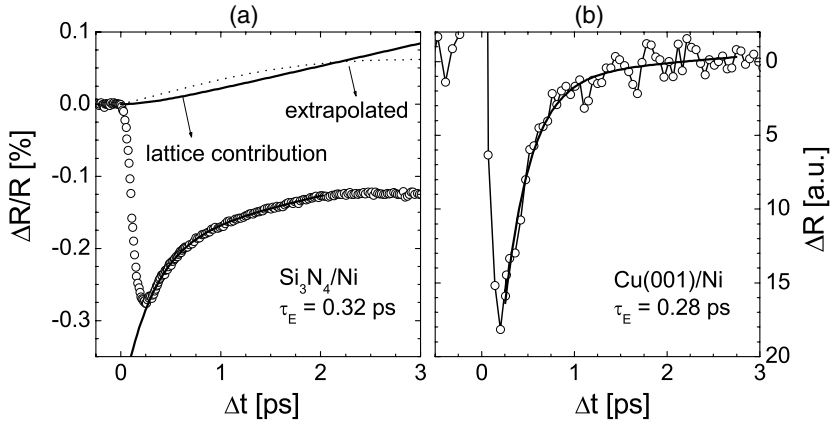

Figure 4. (a) Transient reflectivity measurements on Si/Si_3N_4 (60 nm)/Ni(10 nm)/Cu(3 nm) fitted with equation (6). The solid line labelled 'lattice contribution' represents the lattice term proportional to C. The dotted line is an extrapolation of a fit to the strain wave phenomena on a 2–25 ps interval, shifted vertically to intersect with the origin. (b) Reflectivity data on Cu(001)/Ni using the PEM technique. A coherent contribution shows as a sharp peak near $\Delta t = 0$.

Combining the electron and lattice contributions to ΔR, the transient change in reflectivity for $t \gg \tau_{\mathrm{th}}$ can be described by

$$\Delta R(t)/R = A + B\mathrm{e}^{-\frac{t}{\tau_{\mathrm{E}}}} + C\left(t + \tau_{\mathrm{E}}\left[\mathrm{e}^{-\frac{t}{\tau_{\mathrm{E}}}} - 1\right]\right), \tag{6}$$

with A, B and C appropriate constants. The first two terms describe the contribution of the electron system to ΔR, the last term that of the lattice system. Equation (6) is similar to the function used in [1] to describe reflectivity measurements on gold films.

Figure 4 shows fits of equation (6) to reflectivity data taken on a polycrystalline Si_3N_4/Ni and an epitaxial Cu(001)/Ni sample. It was already shown in the previous section that strain waves play an important role in the polycrystalline sample. From the analysis of the strain wave phenomena it follows that the lattice contribution ΔR_l reaches its first, positive extremum at $\Delta t \sim 3$ ps. To derive the e–p relaxation time, the reflectivity data were fitted up to 2 ps with a positive C to correct for lattice effects. In figure 4(a) the lattice contribution is plotted separately, together with an extrapolation to $\Delta t = 0$ of a fit to the strain wave phenomena on the interval 2–25 ps. The e–p relaxation time is found to be very sensitive to the exact slope of the lattice contribution. The good correspondence with the slope of the extrapolated curve gives confidence that lattice effects are correctly accounted for. However, a considerable uncertainty still remains and values for τ_{E} vary between 0.3 and 0.5 ps, depending on the fit interval and measurement used.

Reflectivity transients measured on the epitaxial sample, plotted in figure 4(b), show a faster decay time $\tau_{\mathrm{E}} = 0.28$ ps. It can be expected that in this all-metallic structure transport effects do have a significant influence, resulting in a more rapid decay of T_{e} by (electronic) heat diffusion into the Cu substrate [10]. The all-metallic structures are therefore less suited to determine the e–p relaxation time, unless one can reliably measure or model the heat transport.

3.4. Temperature dependence

As to the underlying mechanisms for the hot-electron thermalization and e–p energy equilibration, as well as models used for interpretation of the transient reflection experiments (resonant versus non-resonant probing, or even deviations thereof), much is expected to be

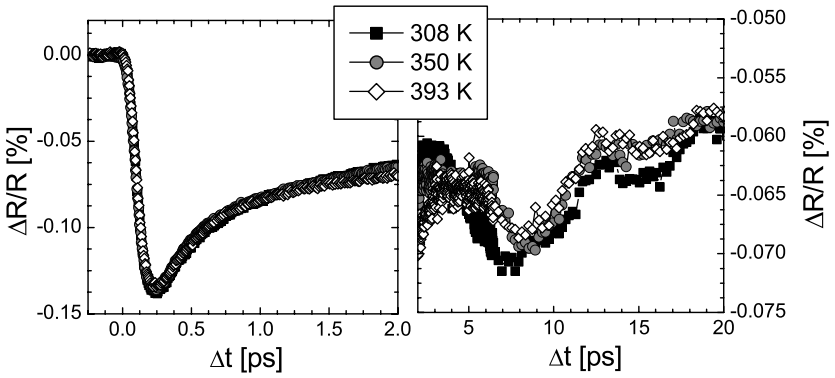

Figure 5. (a) Transient reflectivity measurements on Si/Si_3N_4 (60 nm)/Ni(10 nm)/Cu(3 nm) for three different ambient temperatures. (b) Similar, but showing the long-term dynamics.

learned from inspection of the dependence of the transient profiles on ambient temperature. Results of such a study for the 10 nm Ni film on Si_3N_4 are displayed in figure 5. Since resistive heating of the thin film was performed at ambient condition, it was carefully checked that all transients are fully reversible. For temperatures up to 400 K no degradation of the thin-film structure, e.g. due to oxidation through the capping layer, could be observed.

Figure 5 clearly reveals a surprisingly weak temperature dependence of almost all of the characteristic timescales and amplitudes of the transient reflection. For temperatures between 300 and 400 K, the thermalization time of 0.08 ps, and the position of the extremum, $t_{ex} = 200$ fs are not changed by more than 10%, and no systematic trend could be resolved. Similarly, the e–p energy equilibration, τ_E, is constant over the same temperature interval within 10%. This behaviour was verified several times, also for Ni thin films on other substrates (such as Si/SiO_2). Although interpretation of experiments on the latter substrates turned out to be more complicated due to a larger deposition of heat in the substrate [16], their timescales also hardly varied as a function of temperature. A comparison of these results with predictions by the Fermi-liquid theory and beyond will be presented in section 4.

Not only the timescales, but also the amplitude of the reflection at its first dip after ∼0.2 ps are found to be rather invariant with temperature. Within a resonant probing scheme (cf section 2), which we had to assume to explain the observation of a finite thermalization time, this independency is rather surprising. The resonant scheme means that ΔR is proportional to T_e, and therefore the peak in ΔR should scale with E_P/c_e, where E_P is the pulse energy. Because of the linear temperature dependence of c_e ($\propto T_e$), the peak amplitude should scale inversely proportional with T, i.e. vary by 20% over the temperature range studied. Thus, the foregoing analysis might point to an off-resonant probing scheme, in which case ΔR scales with the excess energy in the electron system, and thereby would be independent of c_e. However, the off-resonant probing would exclude the observation of a finite thermalization time. Therefore we have to conclude that a simple interpretation as in transient reflection experiments on noble metals is not possible, and we need a 'hybrid' interpretation that allows both for a finite thermalization and a signal that roughly scales with the excess energy.

Finally, we mention that also the amplitude of the signal after a few picoseconds is relatively T-independent. In this regime, one expects the amplitude to scale with $(c_e + c_L)$ in the resonant scheme. Also here the weak T-dependence might be interpreted as a signature of probing the excess energy. However, it has to be emphasized that the growing importance of the strain wave effects—that are also seen to be slightly depending on T from figure 5(b)—complicates a quantitative analysis in this regime.

Table 1. Electron–phonon energy relaxation time τ_E on Ni derived from different publications and using equation (6).

Author	τ_E (ps)	Method
Beaurepaire *et al* [5]	1.0	Transmission
Hohlfeld *et al* [6]	0.7–0.8	SHG yield
Hohlfeld [12]	0.6	Reflection
Regensburger *et al* [8]	1.3	SHG yield
Melnikov *et al* [13]	0.4–1.0	SHG yield
Conrad *et al* [17]	0.6–3	SHG yield
This work	0.3–0.5	Reflection

4. Discussion

After sudden laser heating a range of processes take place that change the reflectivity of a material. Our transient reflectivity data on Ni show a delayed extremum at $t_{ex} = 200 \pm 20$ fs that is attributed to the thermalization of the electron gas. This number can be compared with literature values of 260 and 280 ± 30 fs, reported in [5, 6], respectively. However, t_{ex} is not a fundamental parameter. It depends on K_{ee}, τ_E and the length of the laser pulses used. For example, in [5, 6] relaxation times τ_E of, respectively, 1.0 and 0.7 ps are found. In the present work, a shorter τ_E is observed, which is indeed expected to lead to a smaller value for t_{ex}.

The analysis of the reflectivity data is complicated by strong lattice contributions. Separating electron and lattice dynamics, an e–p relaxation time of 0.3–0.5 ps is found for Ni. Literature values on the e–p relaxation time show a much wider spread.

Using equation (6) we reanalysed different data sets published. The resulting values for τ_E are listed in table 1. Transient transmission experiments of Beaurepaire *et al* [5] yield $\tau_E = 1.0$ ps. The SHG data of [6] result in a τ_E of 0.7–0.8 ps, very much independent of the fluence used. From transient reflectivity data on the same structure, published in [12], we find $\tau_E = 0.6$ ps. SHG experiments by Regensburger *et al* [8] yield $\tau_E = 1.3$ ps. The SHG results of Melnikov *et al* [13] on thick polycrystalline Ni films show a strong dependence on the polarization of both pump and probe beam. The authors attribute the spread in relaxation times of 0.4–1 ps to different sensitivities to surface and bulk dynamics, with the faster relaxation attributed to surface dynamics. In [17] the thickness dependence of τ_E is investigated for epitaxial Ni films on Cu(001). The authors report an increasing relaxation time from 0.6 ps for a one monolayer film to 3 ps for six monolayers of Ni, the maximum thickness investigated.

In comparing these values it must be noted that τ_E depends on the electron and lattice heat capacity. Therefore τ_E will also be affected by the excitation density as c_e and c_l are functions of temperature. The large spread in τ_E can however not solely be explained by this effect, as the fluences used in the different reports are very similar. Moreover, we found no significant T-dependence of τ_E.

When performing experiments on bulk crystals, thick films or all-metallic structures, heat diffusion and (ballistic) electron transport can influence the decay time of T_e. Since the majority of the work reported so far in the literature was on optically thick films, or optically thin films on transparent substrates, most of the incompatibilities could be explained by such non-local energy transfer. However, although we tried to qualitatively explain the wide variation of τ_E derived for different structures, we could not obtain a completely consistent explanation. This shows the complexity of the issue, and clearly asks for a more critical selection of structures. We believe that optically thin films on isolating buffer layers, such as employed in the present work, are the best choice for assessing the intrinsic dynamics.

Also extrinsic effects such as morphology could influence the dynamics, complicating a proper comparison. In [6, 8] bulk Ni was used, which in the latter case was single crystalline. The 60 and 100 nm polycrystalline films from [13] can also be considered bulk. The different values of τ_E found in the first two experiments (0.75 versus 1.3 ps) should then be ascribed to structural effects. As mentioned before, the experiments of [13] did not yield a unique value of τ_E. The long relaxation times found in epitaxial monolayer films on Cu are puzzling, and seem to suggest that the dynamics of thin Ni films on Cu is, unexpectedly, not dominated by ballistic or diffusive energy transport into the copper substrate.

As to our T-dependent experiments, we found a number of surprising observations that to the best of our knowledge have not been reported before. The independence of t_{th} on temperature is in striking contrast with the Fermi-liquid theory that predicts a $1/T^2$-dependence (equation (2)), and as such an almost 30% decrease over the temperature interval studied. We also observe no change in τ_E with temperature. Using the two-temperature model [1] the larger electron heat capacity at elevated temperatures ($\propto T_e$) would lead to an increase of τ_E by 20% when heating up to 393 K, assuming a constant electron–phonon coupling. Again, such a strong dependence was not observed.

Deviations from the Fermi-liquid behaviour can significantly modify the T-dependence of t_{th}. In particular, it can be shown that when $\tau_{ee}(E) \propto (E - E_F^{-1})$ (valid for excitation from a localized state below to a continuum of states above E_F), a much weaker $1/T_e$ dependence of the electron thermalization time is found. As such, our T-dependent study of t_{th} would be indicative for a reduced divergence of τ_{ee}. Nevertheless, it is by no means clear that such deviations could also explain the independence of τ_E on T. Clearly, a full understanding of the e–p equilibration is too simplified for materials with a complex band structure near the Fermi level such as nickel.

Finaly, our T-dependent studies made us conclude that measuring transient reflection on Ni thin films at the photon energy used (1.6 eV) provides a hybrid probing scheme in which thermalization can be followed and nevertheless the signal at longer delay times scales with the electron excess energy rather than the electron temperature. One might wonder whether this is a realistic situation. We propose that such a probing may well be obtained if resonance conditions effectively change during the relaxation process. More precisely, it would be required that both the initially created hot electrons and the final thermal distribution of electrons are probed in an off-resonant way. In addition, the thermalized situation should be closer to resonance, or the phase of the optical transitions by interaction with the probe photons should be such that they are more efficiently measured. Given the complicated band structure of nickel with many d-bands close to and crossing the Fermi level does not exclude such a scheme *a priori*. Nevertheless, more detailed spectroscopic studies, as well as a thorough theoretical analysis including full details of the electronic band structure, will be needed to fully validate our schematic conjecture.

5. Conclusions

By carefully engineering samples with a strongly reduced hot-electron transport and heat diffusion out of the laser irradiated volume, we tried to develop a consistent view on the electron and phonon dynamics after laser excitation in ferromagnetic nickel. Using 10 nm nickel thin films on Si_3N_4 insulating barriers, we found a characteristic thermalization time $\tau_{th} = 0.08$ ps, and an e–p energy equilibration time $\tau_E \sim 0.3$–0.5 ps. The thermalization is in reasonable agreement with other recent reports, as well as with simple estimates based on hot-electron lifetimes as measured by 2PPE. Values for the e–p relaxation reported in literature display a very broad spread, 0.5–3 ps. Our experimental estimate lies at the lower bound of

this range. We conjecture that the difference with other reports is due to the fact that almost all other work is based on optically thick films, or films directly grown on metallic substrates. In such cases the experiments will suffer from non-local energy transport, complicating a direct interpretation.

A surprising independence of both τ_{th} and τ_E on ambient temperature was found. As to the thermalization process, a possible explanation may be found in the reduced divergence of the hot-electron lifetime for low kinetic energy. This interpretation is supported by 2PPE data. Although deviations from the naive Fermi-liquid model with a constant density of states may also affect the behaviour of the e–p equilibration, a clear understanding is still lacking. Spectroscopic transient reflection studies as well as more refined theoretical approaches are asked for.

In conclusion, we claim to have measured the intrinsic electron dynamics in ferromagnetic nickel, not hindered by non-local processes and other artefacts. These results are of significant importance for our understanding of electron and phonon dynamics in metallic systems other than the noble metals, and we believe that even more impact can be expected for the field of laser-induced ultrafast magnetization dynamics in ferromagnetic materials. Identification of the spin-relaxation pathways in those experiments is one of the prominent outstanding questions in magnetism today. The magnetic response time in those experiments is a few hundred femtoseconds [5, 16], and thus of the same order as both the thermalization time and the e–p driven energy relaxation time. A reliable input for the electron and phonon dynamics is considered an essential prerequisite for the development of quantitative models for the magnetization dynamics.

Acknowledgment

This work forms part of the research programme of the Dutch foundation for the Fundamental Research on Matter (FOM).

References

[1] Groeneveld R H M, Sprik R and Lagendijk A 1995 *Phys. Rev.* B **51** 11433
[2] Del Fatti N, Voisin C, Achermann M, Tzortzakis S, Christofilos D and Valleé F 2000 *Phys. Rev.* B **61** 16956
[3] Knorren R, Bennemann K H, Burgermeister R and Aeschlimann M 2000 *Phys. Rev.* B **61** 9427
[4] van Hall P J 2001 *Phys. Rev.* B **63** 104301
[5] Beaurepaire E, Merle J C, Daunois A and Bigot J Y 1996 *Phys. Rev. Lett.* **76** 4250
[6] Hohlfeld J, Matthias E, Knorren R and Bennemann K H 1997 *Phys. Rev. Lett.* **78** 4861
[7] Koopmans B, van Kampen M, Kohlhepp J T and de Jonge W J M 2000 *Phys. Rev. Lett.* **85** 844
[8] Regensburger H, Vollmer R and Kirschner J 2000 *Phys. Rev.* B **61** 14716
[9] Oppeneer P M and Liebsch A 2005 at press
[10] Bosco C A C, Azevedo A and Acioli L H 2003 *Appl. Phys. Lett.* **83** 1767
[11] Bauer M and Aeschlimann M 2002 *J. Electron Spectrosc. Relat. Phenom.* **124** 225
[12] Hohlfeld J 1998 *Ultrafast Electron-, Lattice- and Spin-Dynamics in Metals* (Berlin: VWF Verlag für Wissenschaft und Forschung GmbH)
[13] Melnikov A V, Güdde J and Matthias E 2002 *Appl. Phys.* B **74** 735
[14] Guidoni L, Beaurepaire E and Bigot J Y 2002 *Phys. Rev. Lett.* **89** 17401
[15] Koopmans B, van Kampen M, Kohlhepp J T and de Jonge W J M 2000 *J. Appl. Phys.* **87** 5070
[16] van Kampen M 2003 Ultrafast spin dynamics in ferromagnetic metals *Thesis* Technische Universiteit Eindhoven http://alexandria.tue.nl/extra2/200312043.pdf
[17] Conrad U, Güdde J, Jähnke V and Matthias E 1999 *Appl. Phys.* B **68** 511